Atmospheric Environment 352 (2025) 121191

Contents lists available at ScienceDirect

Atmospheric Environment

journal homepage: www.elsevier.com/locate/atmosenv

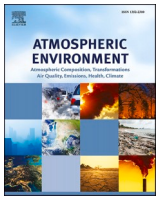

Deducing atmospheric conditions that contribute to elevated pollution events in the Salton Sea Air Basin

Heather C. Lieb [1], Ian C. Faloona [*]

University of California, Davis, United States

HIGHLIGHTS

- Deep stratospheric intrusions and unregulated soil NO_x emissions could be responsible for continued O_3 exceedances.
- Biomass burning, agricultural soil emissions, and wind-blown dust are the main sources of high $PM_{2.5}$ levels in Calexico.
- Extreme PM_{10} levels are mostly associated with strong wind events that occur in the spring and autumn.

ARTICLE INFO

Keywords:
Source apportionment
Air quality management
Atmospheric dynamics
Chemical speciation

ABSTRACT

The Salton Sea Air Basin (SSAB) has struggled to comply with National Ambient Air Quality Standards (NAAQS) for three federally regulated air pollutants: ozone, $PM_{2.5}$, and PM_{10}. Seasonal and diurnal patterns are presented along with their long-term decadal trends to better understand the relationship between the meteorological setting and air pollution levels as well as their deviations. This analysis revealed that ozone exceedances are no longer dominated by regulated NO_x emissions but rather are primarily controlled by regional agricultural soil emissions. These emissions are also likely influenced by stratospheric ozone transport to the deep convective boundary layers unique to the area. Observed peak ozone levels are still ~2–5 ppb lower on weekends indicative of a NO_x-limited regime during the warm season. This implies that local ozone production is directly dependent on NO_x levels, which emphasizes the need to address unregulated sources of NO_x pollution such as those from heavily fertilized, arid agricultural soils. Additionally, strong correlations of $PM_{2.5}$ with NO_x, PM_{10}, and CO, indicate that influences from combustion sources as well as agricultural soils, secondary formation, and mechanical processes are all important sources of $PM_{2.5}$ production in Calexico, the main city of $PM_{2.5}$ non-attainment on the southern border with Mexico. These $PM_{2.5}$ exceedances occur in winter months, when low ventilation accumulates localized $PM_{2.5}$ precursor emissions. Source apportionment of $PM_{2.5}$ was assessed using non-negative matrix factorization of data from the Chemical Speciation Network (CSN) site in Calexico. The CSN data analysis for Calexico identifies biomass burning as the dominant source of high $PM_{2.5}$ concentrations, followed by agricultural soil emissions and wind-blown dust. In the immediate vicinity of the Salton Sea, less frequent $PM_{2.5}$ exceedances seem to be associated with occasional windstorms. Further, analysis of PM_{10} exceedance days indicates that high winds, primarily westerly, are a critical factor, and the low $PM_{2.5}/PM_{10}$ ratios suggest minimal contribution from photochemical or combustion sources. Furthermore, the correlation of PM_{10} with wind speed across various sites underscores the importance of dust resuspension and soil erosion. This comprehensive assessment highlights the complexity of air quality problems in the SSAB. Additionally, it emphasizes the need for targeted and localized air quality management strategies for this region which, despite its low population, suffers some of the worst air pollution impacts in the state of California.

* Corresponding author.
E-mail address: icfaloona@ucdavis.edu (I.C. Faloona).
[1] Now at the California Air Resources Board.

https://doi.org/10.1016/j.atmosenv.2025.121191
Received 20 September 2024; Received in revised form 19 March 2025; Accepted 21 March 2025
Available online 4 April 2025

1. Introduction

The Imperial Valley in Southeastern California, along with the Coachella Valley to the north and the Mexicali Valley to the south, forms the Salton Trough, a nearly 200-km-long tectonic rift extending from the San Gorgonio Pass in Riverside County to the Gulf of California. Air near the surface enters the region through the San Gorgonio Pass and flows southeastward down the valley. However, as the valley widens south of the Salton Sea, westerly airflow transversing the Peninsular Ranges dominates the valley (Figs. 1 and 2). The Salton Sea Air Basin (SSAB) has struggled to meet national ambient air quality standards (NAAQS) (Parrish et al., 2017) despite relatively low population. It is currently classified as nonattainment for ozone (O_3) and coarse particulate matter (i.e., particulate matter with a diameter $\leq$10 μm, PM_{10}). In 2023, the US EPA deemed the SSAB in attainment for fine particulate matter (i.e., particulate matter with a diameter $\leq$2.5 μm, $PM_{2.5}$), however, this attainment was short lived due to the recent lowering of the annual $PM_{2.5}$ NAAQS from 12.0 to 9.0 μg/m^3 (EPA, 2024). For $PM_{2.5}$, the primary annual NAAQS requires $PM_{2.5}$ not to exceed 9.0 μg/m^3 (EPA, 2024), based on an annual mean, averaged over 3 years, while the 24-h NAAQS requires $PM_{2.5}$ that the design value (98th percentile averaged over 3 years) not exceed 35.0 μg/m^3. The NAAQS for ozone requires that the ozone design value (ODV) not exceed 70 ppb; an ODV is defined as the 3-year average of the fourth highest maximum daily 8-h average (MDA8) ozone concentration. Further, there is but one federally regulated NAAQS for PM_{10}, which states that the 24-h average should not exceed 150 μg/m^3 more than once per year on average over 3 years.

Despite its relatively low population compared to nearby urban areas like Los Angeles and San Diego, the region experiences about a dozen ozone exceedance days per year in the south (Calexico) and up to 50–60 in the north (Palm Springs). Additionally, the daily $PM_{2.5}$ NAAQS is frequently exceeded, especially in the south, with daily values often reaching 50–70 μg/m^3 (California Air Resources Board, 2024a). O_3 formation is driven by photochemical reactions involving nitrogen oxides (NO_x) and volatile organic compounds (VOCs) in sunlight. There are various sources of O_3 precursors, including mobile sources (e.g., vehicles and trucks), stationary sources (e.g., industrial activities), and biogenic sources (e.g., soils and wildfires). Sources of $PM_{2.5}$ in the SSAB include agricultural activities, such as tilling and burning, as well as industrial emissions and vehicle exhaust (Dessert, 2018b).

Air pollution is the second leading risk factor for premature mortality globally (Institute for Health Metrics and Evaluation, 2021). Both acute and chronic exposure to these air pollutants have been associated with negative health effects, including respiratory and cardiovascular issues and diseases (Al-Hemoud et al., 2018; Caiazzo et al., 2013; Dominici et al., 2006; Hao et al., 2015; Kim et al., 2020; Madl et al., 2010). In fact, during the peak of the pandemic, Imperial County suffered from the highest mortality and contraction rates from COVID-19 per capita in the

Fig. 1. CARB sites used for the meteorological and air pollution climatology studies. Note that Imperial Valley sites begin at Bombay Beach and move south. The sites north of the Salton Sea are within the Coachella Valley, *except for Banning*, which is a part of the South Coast Air Basin but is used as a reference point for the study. Mexicali, MX was also included as a reference point.

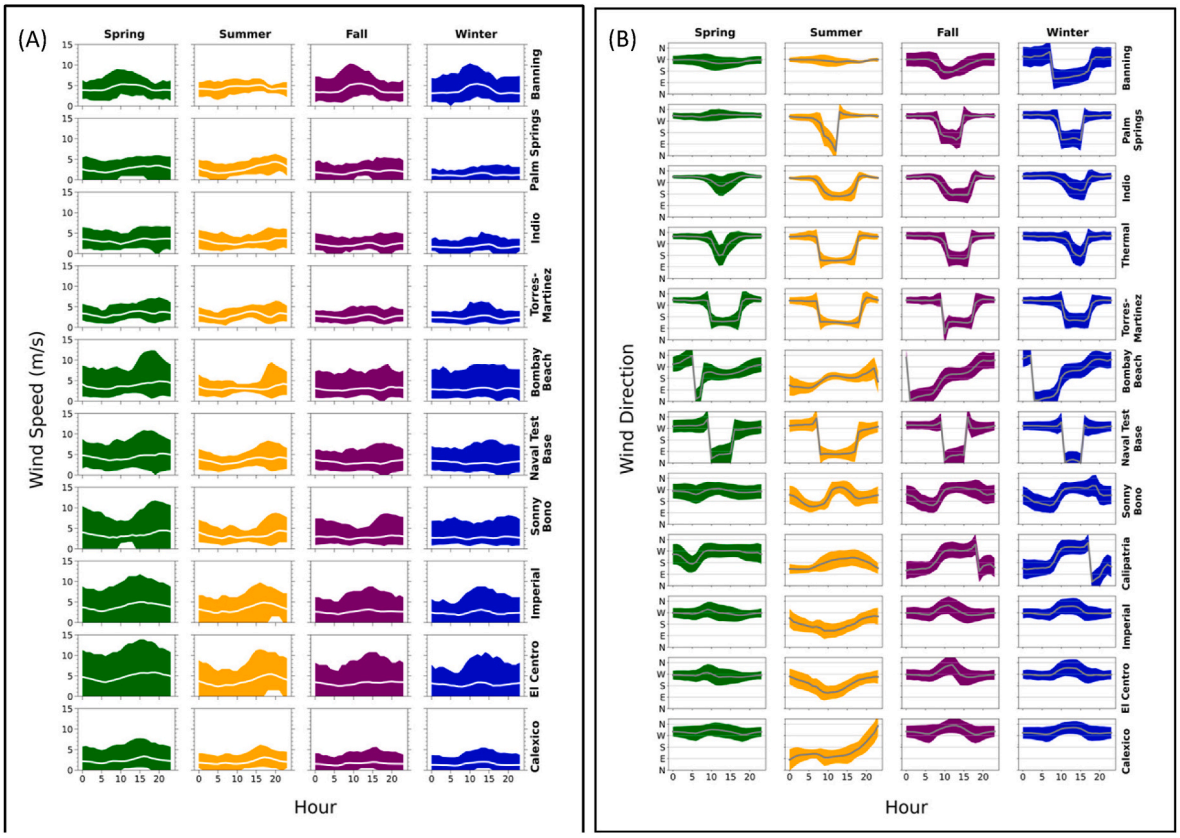

Fig. 2. (A) Seasonal diurnal scalar average wind speed. White lines indicate the seasonal average while the colored area represents the upper 95th percentile and lower 5th percentile. (B) Seasonal diurnal wind direction. Grey lines indicate the seasonal average while the colored area represents the standard deviation of the wind direction.

state (The New York Times, 2023), a consequence believed to be partly due to the chronic exposure to air pollutants (Borro et al., 2020; Garcia et al., 2022; Johnston et al., 2019; Marian et al., 2022). In addition, this region is characterized by high rates of poverty, language barriers, impaired water quality, and various other environmental and socio-economic injustices (OEHHA, 2023).

The conventional, received wisdom seems to be that the region's ozone and $PM_{2.5}$ issues are dominated by exogenous sources: in the Imperial Valley, pollutants come from the greater San Diego/Tijuana area and the border town of Mexicali, while in the Coachella Valley, pollutants are carried from the Los Angeles Basin (EPA, 2022, 2023; Mendoza et al., 2010; Shi et al., 2009; Watson and Chow, 2001). However, despite statewide efforts to reduce pollution sources in surrounding urban regions, especially due to the efforts of the Clean Air Act to reduce combustion sources, ozone and $PM_{2.5}$ reductions in the SSAB have been minimal during the last decade, indicating that localized sources may be influencing their continued nonattainment. In fact, many of the remaining areas in California struggling to comply with current ozone and $PM_{2.5}$ air quality standards are rural, agriculturally active regions, therefore, the sources dominant in these areas must be considered in future management practices (Almaraz et al., 2018; Freedman et al., 2020; Oikawa et al., 2015; Trousdell et al., 2019; Wang et al., 2023).

Warm year-round temperatures make the Imperial Valley one of the most productive agricultural regions in California, the largest year-round irrigated area in the nation, with an estimated economic output of over two billion dollars annually (California Department of Food and Agriculture, 2023). In addition, the Coachella Valley is home to 135 golf courses which require regular seeding, fertilization, and irrigation. Consequently, the SSAB is home to some of the largest soil emissions of nitrogen oxides ($NO_x = NO + NO_2$) (Almaraz et al., 2018; Lieb et al., 2024; Oikawa et al., 2015; Parrish et al., 2017), a precursor to both ozone and particulate nitrate. Aside from ongoing cropping activities, surplus nitrogen inputs in the region, which have increased 10-20-fold over the past century (Byrnes et al., 2020), could also impact these emissions. In addition, agricultural tilling is a source of particulate matter in the region (Dessert, 2018a). Despite mounting evidence for the significance of soil NO_x emissions in the region (Lieb et al., 2024), no effort has been made to address this issue. Further, this region is home to the Salton Sea, a saline lake at risk of desertification due to increasing imbalances between inflows and evaporation that have resulted in water level declines by about 13 m since the 1950s. This drastic change has resulted in 124 km^2 of newly exposed lakebed, which threatens to exacerbate air pollution and public health concerns due to the potential for increasing emissions of particulate matter (Abman et al., 2024; Johnston et al., 2019; Jones and Fleck, 2020; Pacific Institute, 2024). The production of soil NO_x and its resultant secondary particulate matter are projected to increase due to increased agricultural activity (fertilizer use) and climate change (warmer soil conditions). This puts these already disadvantaged communities at higher risk of respiratory and cardiovascular damage. Therefore, addressing both meteorological phenomena and pollution sources that contribute to poor air quality in the region is crucial.

Moreover, PM_{10} is often generated from natural events like dust storms, which are common in the arid climate of the SSAB, and are further exacerbated by various anthropogenic activities such as diminished agricultural runoff into the Salton Sea (Abman et al., 2024). Additionally, human activities, including agricultural operations, construction, and unpaved road/ATV travel, contribute to elevated PM_{10} levels. The exposed lakebed of the Salton Sea, due to receding water levels, has become a significant source of dust, further aggravating PM_{10} pollution (Frie et al., 2017; Johnston et al., 2019; Jones and Fleck,

2020). These particles can be inhaled and deposited throughout the upper airways of the lungs, which can adversely affect respiratory and cardiovascular health (California Air Resources Board, 2023). Negative health implications to PM_{10} exposure can include reduced lung function (D'Evelyn et al., 2021); worsening of asthma and other respiratory diseases; increased hospitalization and emergency department visits; faster disease progression; and reduced life expectancy (California Air Resources Board, 2023). The episodic nature of PM_{10} pollution, driven by both natural and human factors, makes regulatory measures challenging.

To understand the components that influence air quality exceedances, it is important to first understand the region's typical atmospheric conditions. Diurnal, seasonal, and annual trends are developed in this work for various air pollutants and meteorological conditions from the years 2009–2023 using existing air monitors from the California Air Resources Board (CARB). This exercise is used to understand the relationship between monitored air pollutants and meteorological conditions using Pearson's correlation coefficient (R^2) and the slope (m). Additionally, normalized anomalies were calculated for days that exceeded the National Ambient Air Quality Standards (NAAQS) for ozone, $PM_{2.5}$, and PM_{10}. Moreover, data from the Chemical Speciation Network site located in Calexico, where $PM_{2.5}$ exceedances are most concentrated, was used to apportion sources of $PM_{2.5}$ using non-negative matrix factorization (NMF). Clarifying the components that influence poor regional air quality will allow for improvement in measurement practices.

2. Methods

2.1. Trend assessments

To investigate regional air quality and meteorological trends, hourly data was obtained from the California Air Resources Board's (CARB) air quality and meteorology data query tools for the years 2009–23 (except for $PM_{2.5}$, which only had sufficient data from 2014 to 23) (California Air Resources Board, 2024a, 2024b). The meteorological parameters under investigation were temperature, scalar wind speed, U and V wind components (westerly/zonal and southernly/meridional, respectively), vector mean wind direction, and specific and relative humidity, while the air pollutants under analysis included O_3, $PM_{2.5}$, PM_{10}, CO, and NO_x.

2.2. Normalized anomaly (σ) calculations

Sites from the CARB air monitoring network (Fig. 1) were used to calculate normalized anomalies (σ) for various meteorological and pollution parameters of ozone, $PM_{2.5}$, and PM_{10} concentrations. Because of the strong seasonal (monthly) dependence of most AQ and meteorological parameters, we present deseasonalized normalized anomalies, calculated using Equation (1):

$$\sigma = \frac{x - \bar{x}}{sd} \tag{1}$$

Where x represents the 24-h averages for each variable, $\bar{x}$ is the monthly average over the 14-year period, and anomalies are normalized by the monthly-averaged standard deviation (sd) across the 14 years. The normalized anomalies were primarily analyzed on days that exceeded the NAAQS (70 ppb, 35 μg/m^3, and 150 μg/m^3 for ozone, $PM_{2.5}$, and PM_{10}, respectively) to identify any significant meteorological or pollutant outliers that occurred during these extreme pollution episodes. We consider the normalized anomalies to be somewhat significant if $\sigma \geq 0.4$ (or $\sigma \leq -0.4$) and very significant if $\sigma \geq 1$ (or $\sigma \leq -1$); these values can be found in Tables S3, S5, S6a, and S6b. Equation (2) below shows the calculation for standard error (SE) where sd (shown in Tables S3, S5, S6a, and S6b), is the standard deviation and n represents the number of available datapoints for a given variable.

$$SE = sd/\sqrt{n} \tag{2}$$

Because of the strong diurnal behavior of the thermally forced circulations in the SSAB, we also use an analogous (non-normalized) de-diurnalized ozone value in our pollution rose analysis of Section 4.2.

2.3. Correlation coefficient (R^2) calculations

Pearson's correlation coefficients (R^2) were calculated for ozone and the aforementioned meteorological and pollutant components. This parameter was calculated between ozone MDA8 and T_{max}, daytime scalar average wind speed, daytime U and V components, and 24-h average relative and specific humidity, $PM_{2.5}$, PM_{10}, NO_x, and CO. The calculations were only performed for the months of April through September, since ozone formation peaks during the afternoon and in the warmer months. Coefficients for $PM_{2.5}$ and PM_{10} were not significant and therefore were not reported. Statistically significant correlation coefficients are indicated by a p-value of less than or equal to 0.05, and these values can be found in Tables S4a and b.

2.4. Chemical speciation and source apportionment of $PM_{2.5}$

$PM_{2.5}$ concentrations in the SSAB are highest in Calexico, therefore to better identify sources that contribute to $PM_{2.5}$ production in the SSAB, data from the Chemical Speciation Network (CSN) in Calexico, CA was utilized (US EPA, 2016) from 2009 to 2023 (one full 24-hr sample approximately every 6 days for a total of 718 data points). A continuous time series was constructed, using the corrections described in Malm and Hand (2007) based on EPA recommended IMPROVE protocols (Malm and Hand, 2007). Specifically, dry $PM_{2.5}$ mass concentrations are computed using the following equations:

$$PM_{2.5} = 1.37[SO_4^{2-}] + 1.29[NO_3^-] + [POM] + [EC] + [Soil] + [Sea\ Salt], \tag{3}$$

$$POM = 1.4[OC], \tag{4}$$

$$Soil = 2.2[Al] + 2.49[Si] + 1.94[Ti] + 1.63[Ca] + 2.42[Fe] \tag{5}$$

$$Sea\ Salt = 1.8[Cl^-] \tag{6}$$

where sulfate (SO_4^{2-}) is assumed to be fully neutralized to ammonium sulfate ($(NH_4)_2SO_4$), nitrate (NO_3^-) is assumed to be in the form of ammonium nitrate (NH_4NO_3), and organic carbon (OC) is included as particulate organic matter (POM). The EPA describes the calculation of organic carbon (OC) and elemental carbon (EC), since there are multiple measurements of each, and the following equations are used:

$$OC = OC1 + OC2 + OC3 + OC4 + OP \tag{7}$$

$$EC = EC1 + EC2 + EC3 - OP \tag{8}$$

where OP represents pyrolyzed organic carbon. OP is measured using two methods: thermal optical reflectance (TOR) and thermal optical transmittance (TOT). TOR measures the change in reflectance of the sample surface as it is heated, while TOT measures the change in transmittance, or light passing through, as the sample is heated. Both methods of measurement are necessary to fully depict the OP concentrations since surface reflectance might underestimate OP in the sample's interior, while transmittance might overestimate it if the interior changes are more pronounced than the surface. Therefore, "OC" and "EC" are reported as OC_TOR, OC_TOT, EC_TOR, or EC_TOT depending on the OP measurement. These measurements give strikingly different results, so defining them separately is important. This method of reconstructing $PM_{2.5}$ has good agreement with measured $PM_{2.5}$ concentrations, with a slope of 1.01 and R_2 of 0.83 (Fig. S1).

In addition to chemical speciation, non-negative matrix factorization (NMF, a python package) was used for source apportionment of $PM_{2.5}$.

Source apportionment aims to extract the source contributions and profiles of p factors from the speciated concentrations of $PM_{2.5}$ using mass balance analysis, which can be written to account for all m chemical species in the n samples as contributions from p independent sources.

$$x_{ij} = \sum_{k=1}^{p} g_{ij} f_{kj} \tag{9}$$

Here, x_{ij} is the jth chemical species concentration measured in the ith sample, g_{ik} is the airborne contribution of material from the kth source contributing to the ith sample, and f_{kj} is the concentration of the jth species from the kth source (Hopke, 2016). The CSN data was used in this NMF to determine the sources of $PM_{2.5}$ in Calexico. Once the factorization was completed and the sources were identified, we then looked at the 90th percentile and 98th percentile days to see the dominate sources of pollution. Although the data is limited to collections every 6 days, this analysis will allow for a better understanding of which sources may result in nonattainment days, allowing for policy makers to focus on these sources in regulatory decisions.

3. Regional wind patterns

Establishing the typical wind patterns helps clarify the mesoscale meteorological influences on regional air pollution transport and processing and can aid in understanding the interregional impacts of pollution events. Monthly wind roses have been prepared using wind data from ten of the California Air Resources Board sites during 2009–2023, showing monthly averaged wind patterns (Figs. S2a–j). Due to the presences of the large body of water at the center of the valley, separating Imperial and Coachella Valleys, a sea/lake breeze is regularly observed and represents one of the dominant influences on diurnal wind patterns within the valley (Fig. 2), especially nearest the sea. Further from the seashore a larger-scale valley mountain flow is evident, which is reinforced by monsoonal flow from the Gulf of California during the warmest months. Because of the thermally forced nature of these circulations, they are especially pronounced in the warm season.

Beginning in the Southern Imperial Valley, there are three main meteorology sites in Calexico, El Centro, and Imperial (refer to Fig. 1). Calexico is located about 65 km south-southeast of the Salton Sea along the Mexican border and experiences westerly and northwesterly winds (Fig. S2a), the strongest of which are observed during the late winter and spring (strong synoptic forcing). A wind reversal occurs in the warmest months when southeasterly flow strengthens and dominates due to the North American monsoon (Adams and Comrie, 1997) bringing moist air from the Gulf of California into the valley. El Centro is located north-northwest of Calexico and westerly winds prevail year-round. In early spring, the westerlies strengthen (peaking in May) until early summer, when the monsoonal flow from the southeast develops during the warmest months of July and August. The effect of the monsoonal flow is reduced in the evening (Fig. 2B), when the winds veer to south-westerly with nighttime drainage flows on the west side of the valley likely strengthened by prevailing westerlies. El Centro experiences the most intense westerly wind events during the spring and early summer, with hourly wind speeds exceeding 9 m/s around 20 % of the time. It is likely that the high wind speeds result from downslope acceleration of flow channeled through the lowest point in the north-south transect of the Peninsular Range, referred to as the “El Centro Gap” (Evan, 2019). Additionally, Imperial, the meteorology site located just 7 km north of El Centro, experiences less intense wind gusts, but otherwise the general wind patterns are comparable to El Centro and Calexico. CARB sites located along the perimeter of the Salton Sea are in Sonny Bono, Bombay Beach, the Naval Test Base, and on the Torres-Martinez tribal land. Winds in these regions are largely characterized by daytime sea breezes from the Salton Sea followed by nighttime downslope/downvalley winds and land breezes.

The Coachella Valley is comprised of two major CARB sites: Indio and Palm Springs. Indio is northwest of the Salton Sea, and Palm Springs is located near the northernmost point of the Salton basin just on the east side of the San Gorgonio (i.e., Banning) Pass, but sheltered by the San Jacinto Mountains to the west. Both sites observe generally weaker winds dominated by northwesterlies channeled in through the pass but exhibit a daytime up-valley wind except during the spring when the channel flow is strongest due to the background synoptic forcing. Lastly, Banning, in the San Gorgonia gap, is dominated by westerlies throughout the year. These westerlies are driven by the large-scale pressure gradient channeled through the terrain (Fig. S2j), except during the wintertime high pressure events which can reverse the pressure gradients pumping SSAB air out into the LA basin.

4. Results and discussion

It is crucial to understand the environmental factors that contribute to O_3, $PM_{2.5}$, and PM_{10} pollution, especially the long-term, seasonal, and diurnal trends. Fig. S3 shows the monthly probability of MDA8, $PM_{2.5}$ and PM_{10} daily NAAQS exceedances (70 pbbv, 35 μg/m^3, and 150 μg/m^3, respectively) at each site, illustrating the seasonal patterns of air pollution extremes in the SSAB. This figure shows the highest likelihood of ozone exceedances in June at most sites, but also July in Banning (which is downwind of the LA air basin). They are more than twice as prevalent in the Coachella Valley relative to the Imperial Valley. Note also that many sites (Niland, El Centro, and Indio) have the second highest O_3 exceedance probability in May (late spring). Fig. S3 further shows that winter months in Calexico and spring at the Naval Test Base are most likely to have daily $PM_{2.5}$ exceedances. Furthermore, while there is a lot of variability between sites for PM_{10} exceedances, sites around the Salton Sea are most likely to experience PM_{10} exceedances, especially in spring and fall.

4.1. Ozone

Ozone production is seasonal by nature, with the highest near-surface concentrations usually observed in the summer months due to the peak in actinic fluxes, more frequent air stagnation under high pressure systems, increased emissions of anthropogenic and biogenic VOCs, as well as the thermal degradation of PAN (Porter and Heald, 2019). In polluted environments, PAN is a thermally equilibrated trace gas that serves as a significant temporary sink for NO_x. Photochemical production of ozone is also dependent on temperature-dependent chemical reaction rates. However, in regions of the US with strong temperature-ozone correlations, the temperature-dependent chemistry (e.g. PAN equilibrium) and emissions have been shown to make up less than half of the relationship, while mass transport yields the majority (~60 %) (Kerr et al., 2019; Porter and Heald, 2019). Kerr et al. (2019) also found regions in the southern US near bodies of water, such as the lower Mississippi Valley, the Texas Gulf Coast, and the Salton Sea, to exhibit very weak correlations between T and O_3, very similar to our findings tallied in Tables S3 and S4 ($0.01 < R_2 < 0.11$). Here, other factors are more important in determining the highest ozone concentrations. For example, stratospheric intrusion events are particularly influential in the southwestern US (Zhang et al., 2020; Škerlak et al., 2014), which may explain why the second highest month of O_3 exceedance probability is May, closer to the peak in the stratospheric influx of O_3, for some of the sites in the interior of the SSAB (e.g., Indio & El Centro, Fig. S3).

The persistence of elevated near-surface ozone concentrations has been an issue for decades, originally dominated by anthropogenic sources in the urban regions of California (Haagen-Smit, 1954). Air quality regulations resulted in large reductions in the anthropogenic emissions of ozone precursors (mostly NO_x and reactive organic gases, ROG, or non-methane volatile organic compounds, NMVOC), exponentially lowering the ambient ozone concentrations over the decades

(Parrish et al., 2017). However, several rural regions of California still exceed the 2015 NAAQS for ozone, including the Salton Sea Air Basin (Parrish et al., 2017, 2024). With reference to Table S1 and Fig. 3 (ODV), it is apparent that there has been little to no improvement in ODV concentrations over the last 5–10 years in the SSAB (with the possible exceptions of Niland and Indio). This lack of improvement indicates that regulated, anthropogenic combustion sources are likely no longer the determining factor in ozone nonattainment. While Niland and Indio's ozone pollution seems to be improving over the past decade, the rate of ozone decline has slowed at all other sites (especially since ~2016), and a positive slope is observed in Calexico and Banning since about 2011–2015, which has also been observed in Southern California Air Basin more broadly (Wu et al., 2023). Unregulated sources like agricultural NO_x emissions and managed landscapes like golf courses, or natural phenomena like stratospheric intrusion and subsidence on the lee side of the Pacific high, may be significantly responsible for continued nonattainment challenges (Carrow, 1997; Parrish et al., 2017, 2025; Zhang et al., 2020; Škerlak et al., 2014). Referring to Table S2 and Fig. S4, which show trends in annual NO_x averages from 2009 to 2023, it is apparent that, outside of Calexico, the regulatory decline in NO_x concentrations is mostly absent since 2016. This indicates that the threshold of reduced mobile source emissions has likely been approached and unregulated sources of NO_x need more focus to reach attainment goals. Further investigation is necessary to understand the impact of mass transport and to confirm whether stratospheric intrusion is a dominant factor. However, several studies have implied that soil NO_x emissions in the SSAB are massively consequential (Almaraz et al., 2018; Lieb et al., 2024; Oikawa et al., 2015; Wang et al., 2021) and will need to be addressed in order to further air quality and environmental justice goals in the region.

4.2. Normalized anomalies and correlation coefficients (R^2) for ozone

Six sites from CARB were used to calculate normalized anomalies and correlation coefficients for ozone and various meteorological and pollution parameters. Three sites belong to the Imperial Valley (i.e., Calexico, El Centro, and Niland), and three sites belong to the Coachella Valley (i.e., Indio, Palm Springs, and Banning, although Banning is not a part of the SSAB). The number of exceedance days, normalized anomalies, and SE for each site during the 2009–2023 timeframe is shown in Table S3. Additionally, correlation coefficients (R^2) were calculated for ozone and various meteorological and air pollutant components for the months of April through September (Tables S4a and b).

Based on the analysis of normalized anomalies in Calexico (Table S3), ozone exceedance days are characterized by warmer than average temperatures, low (more northerly) wind speed, and low humidity (68th, 23rd, and 34th percentiles of the normalized anomaly values, respectively). Because of the reasons outlined in Section 4.1, it is generally expected to see ozone exceedances occurring when temperatures are high. However, Table S4 shows that the linear relationship between MDA8 is only weakly correlated with the maximum daily temperature from April–September therefore temperature is not the dominant factor influencing day-to-day ozone extreme values in the region. These results were comparable to those reported in Kerr et al. (2019). We interpret the average deviations of T, wind speed/direction, and humidity to be evidence of atmospheric dynamics and temperature-dependent precursor emissions influencing elevated levels of ozone on synoptic time scales (longer than one day yet shorter than the monthly averages used in calculating the normalized deviations). For example, low humidity is consistent with synoptic-scale deep stratospheric transport into the deep boundary layers common in the US southwest as illustrated in Škerlak et al. (2014) and discussed in Section 4.1.

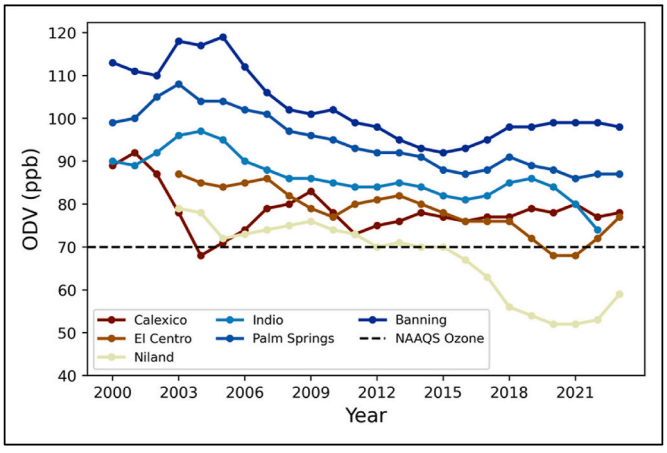

Fig. 3. Ozone design values (ODV) for the six CARB sites in the Salton Sea Air Basin from 2000 to 2023. The NAAQS for ozone is denoted by the dashed black line at 70 ppb.

Southeasterly monsoonal winds are most frequent during the warmest months in the Imperial Valley (July/August, which have lower exceedance probabilities than May/June when the winds are westerly/northwesterly, Fig. S3). However, conditions of stagnant and dry air (Table S3) indicate that ozone exceedances are not predominantly related to transport from Mexicali, Mexico, and by extrapolation moist air masses from the Gulf of California. This is a very consequential finding because international transport is often assumed to be the primary contributor to ozone pollution in the Imperial Valley (EPA, 2022). Fig. 4 shows that hourly ozone deviations from the diurnal means in Calexico are larger on days when winds are predominantly northwesterly (Table S3 also shows the correlation with northerly, $V < 0$, winds). Further, CO concentrations on ozone exceedance days in Calexico are average, neither elevated nor low, which may indicate that traditional combustion processes are not the dominant source of ozone precursors.

Looking at the weekday vs weekend differences in ozone levels, or the "weekend effect", helps to understand the ozone production sensitivity to NO_x reductions and the role that vehicle emissions play in ozone levels. Typically, sites dominated by background ozone (e.g., unregulated anthropogenic sources, biogenic sources, and baseline ozone) or long-range transport have similar weekday/weekend O_3, while sites dominated by local/regional anthropogenic O_3 sources do not (Heuss et al., 2003). Heuss et al. investigated the weekend effect for Calexico during ozone season (April–September) from 1996 to 1997, which showed that the region observed lower O_3 on weekends. This indicates a NO_x-limited regime in which the production of ozone is principally limited by the availability of NO_x rather than that of VOCs. In comparison, Fig. S5A shows the weekend effect for Calexico during ozone seasons from 2014 to 2023, some two decades later, also evincing a consistent trend of lower O_3 on weekends. Thus, it appears that Calexico is still NO_x-limited, and the average Sunday diurnal cycle has not changed much in concentration, although weekday concentrations of ozone have decreased by 5–10 ppb since the late 90's. Therefore, we see that the reduction of mobile source emissions, mostly NO_x from heavy duty diesel vehicles (Marr and Harley, 2002), does reduce the average ozone concentration during the weekend. Fig. S6A shows the observed decline in NO_x concentrations on Sundays in comparison to weekday concentrations. El Centro observes the most ozone exceedances in the Imperial Valley, and like Calexico those high ozone days are characterized by relatively warm, weak and more northerly wind, and dry conditions. However, unlike Calexico, O_3 exceedances in El Centro co-occur with high NO_x, $PM_{2.5}$, CO, and $PM_{2.5}/PM_{10}$ concentrations (82nd, 80th, 79th, and 71st percentiles, respectively). El Centro has a similar weekend effect to Calexico (Fig. S4B), however, because El Centro's ozone exceedances are characterized by high NO_x, $PM_{2.5}$, and CO, this may indicate that some photochemical processes are significant, which might include local domestic mobile source emissions and agricultural equipment (Li et al., 2015).

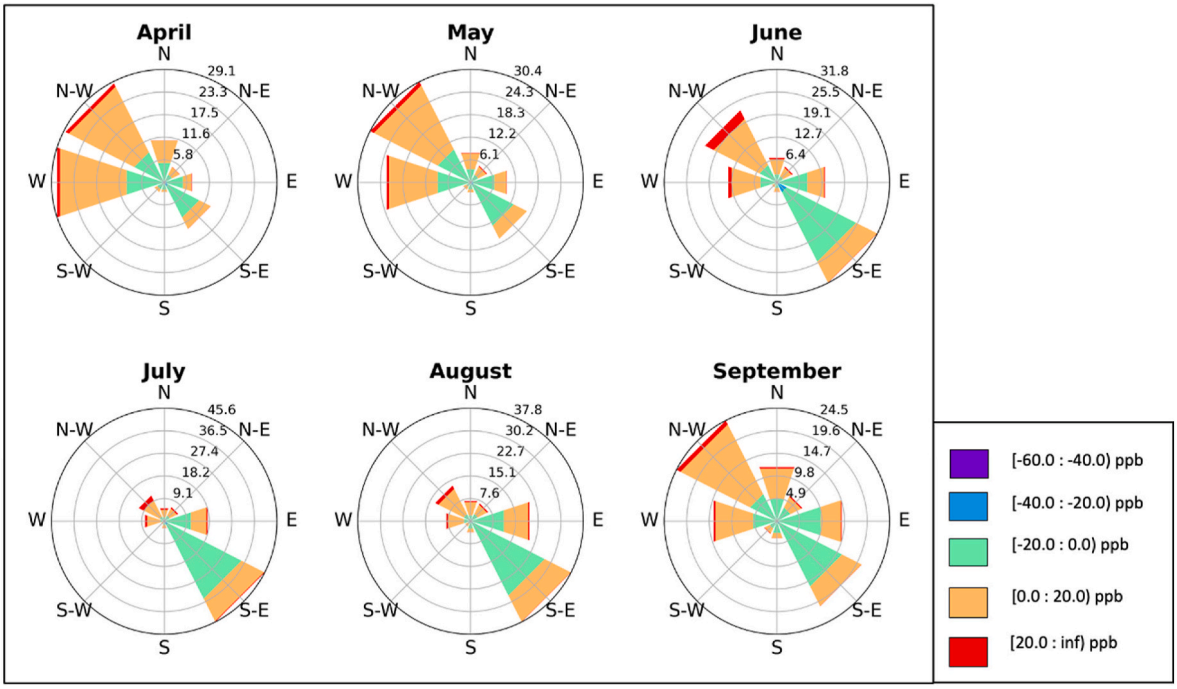

Fig. 4. Ozone pollution roses for Calexico during June–September. The colors represent *hourly ozone deviations* from the mean. (For interpretation of the references to color in this figure legend, the reader is referred to the Web version of this article.)

Nonetheless, Imperial County is agriculturally active year-round, meaning elevated NO_x emissions may result from soil emissions of NO. Agricultural NO_x emissions have not been regulated despite many studies that have shown their significance in agricultural areas, especially the Imperial Valley (Almaraz et al., 2018; Lieb et al., 2024; Luo et al., 2022; Oikawa et al., 2015; Sha et al., 2021). Agricultural soil NO_x emissions are principally dependent on fertilizer inputs, soil moisture, and temperature. The temperature dependence is believed to be exponential up until about 30–40 °C where emissions are observed to plateau due to heat stress (Wang et al., 2021; Yienger and Levy, 1995). A recent study by Lieb et al. (2024) estimated that agricultural soils contribute 34.7 % on average to the Imperial County NO_x budget. The sensitivity of ozone production to NO_x [δO_3 MDA8/δNO_x] based on the weekend effect (Figs. S4–S5) in Calexico is ~1 ppb of O_3 MDA8 per ppb of afternoon NO_x. The average NO_x concentration from April–September is 6.1 ppb, meaning about 2.1 ppb NO_x originate from agricultural soils according to the Lieb et al. (2024) study. In response to soil NO_x production then, about 2.2 ppb MDA8 O_3 is elevated on average during ozone season. In a NO_x-limited regime, increases in NO_x concentrations from agricultural activity, say due to increasing N fertilizer amendments and/or rising soil temperatures, can lead to higher concentrations of ozone, pushing the region further away from attaining the NAAQS.

Modeling studies have shown that stratospheric contribution to the tropospheric ozone budget is similar in magnitude to net photochemical production (Roelofs and Lelieveld, 1997; Stevenson et al., 2006). In fact, some stratospheric mass transport happens as a result of deep stratosphere-troposphere exchange (STE), when ozone is transported from the stratosphere into the atmospheric boundary layer (Škerlak et al., 2014, specifically their Fig. 5). These events have a strong seasonal dependence and peak in the spring in the midlatitudes but occur throughout the year and are a particularly important factor in ozone exceedances in the Southwestern US and the SSAB (Parrish et al., 2024; Zhang et al., 2020). Stratospheric air is characterized by very low water vapor, and drier than normal conditions are observed at most of the sites on ozone exceedance days, with negative correlations observed for specific humidity in the summer months (Tables S4a and b). According to Škerlak et al. (2014), the boundary layers that are most impacted by

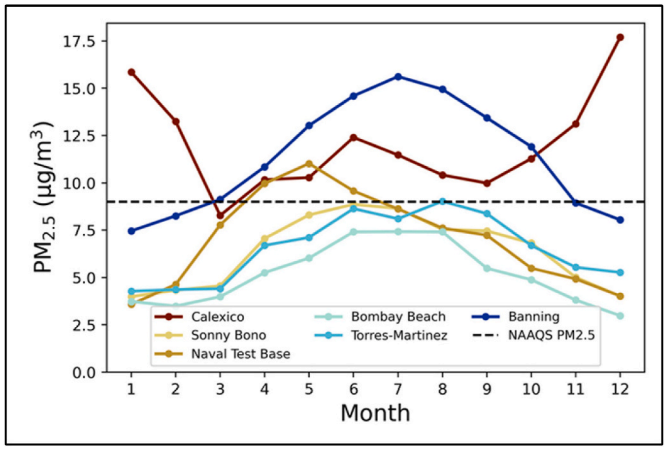

Fig. 5. Monthly average values for $PM_{2.5}$ were calculated using 24-h average $PM_{2.5}$ concentrations for 2014–23 (as available). The 1-year 2024 National Ambient Air Quality Standard (NAAQS) is denoted by the black dashed line.

stratospheric intrusions are within the US southwest and the Tibetan Plateau, specifically in subtropical deserts near regions of high orography. These inputs tend to reach a maximum when the tropopause ozone concentrations are highest and baroclinic instabilities are most common, which happens in the late spring/early summer. The SSAB is broadly downwind of the Peninsular and Transverse Ranges, and much of those ranges elevations are between 1.5 and 3 km in height (Evan, 2019). The proximity of these mountain ranges to the desert creates a mountain valley circulation that promotes deep tropospheric mixing. High orography and low air density combined with intense solar heating leads to deep convective boundary layers, and the deeper the boundary layers, the farther the vertical mixing reaches into the free troposphere, bringing down these ozone concentrations enhanced from stratospheric inputs. In addition, subtropical deserts observe the largest summertime boundary layer heights due to dry convection, again mixing down higher ozone at higher elevations. These factors combined with the

strong subsidence associated with mountain-valley circulations (and the Pacific High anticyclone) makes the Salton Sea Air Basin a prime location for deep STE and exceptionally high "background" ozone concentrations.

In the Coachella Valley, ozone exceedances are much more frequent, but without strong correlations (Table S4b) or significant normalized anomalies (Table S3), it is difficult to identify specific conditions that influence ozone exceedance events. It is likely that ozone exceedances in the Coachella Valley are a mixture of anthropogenic combustion sources, both local and interregional, as well as background ozone and biogenic sources (i.e., agriculture, golf courses, fertilized lawns). Agricultural emissions may be the most influential at the Indio monitoring site due to its proximity to the agriculturally active eastern Coachella Valley. Weekend effects in the Coachella Valley at Indio and Palm Springs O_3 monitoring sites also show a NO_x-limited regime (Figs. S5C and D). Based on sampling $^{15}N/^{14}N$ ratios at a site near Thermal, Lieb et al., 2024 estimated that agricultural soils contribute 21.0 % on average to the Coachella Valley NO_x budget. The sensitivity of ozone production to NO_x [δO_3 MDA8/δNO_x] based on the weekend effect (Figs. S4–S5) in Palm Springs is ~7 ppb of MDA8 O_3 per ppb of NO_x, much stronger than in Calexico. The average afternoon NO_x concentration in Palm Springs during ozone season is 2.4 ppb, meaning about 0.5 ppb originates from soils. In response, we expect to see an elevation of 3.5 ppb MDA8 O_3 on average from this unregulated source.

To summarize, ozone pollution in the Imperial Valley seems to result primarily from localized emissions and depend strongly on temperature-dependent precursor emissions and atmospheric dynamics. While interregional transport from Mexicali, Mexico is a source, ozone concentrations that deviate higher than average during ozone season dominate when northwesterly winds are observed, further suggesting that basin-wide sources of ozone and its precursors strongly influence the air quality. Furthermore, the Coachella Valley observes many more ozone exceedance days than the Imperial Valley, in part due to proximity of highly urbanized areas (the outlet of the LA basin), with agriculture and managed landscapes (e.g., golf courses) likely contributing to the production of ozone and its precursors. The SSAB is a NO_x-limited regime during the warm season, meaning that increases in NO_x emissions will increase the production of ozone, causing the NAAQS for ozone to be pushed further away from attainment. To mitigate the exacerbation of these conditions, unregulated sources of ozone precursors (e.g., agriculture, golf-courses) should be studied further and considered for future regulatory action.

4.3. $PM_{2.5}$

Imperial County has recently been reviewed by the EPA, deeming the county in attainment for the 2012 p.m.$_{2.5}$ standard by its December 31, 2021 "Moderate" area attainment date. However, this attainment was short lived due to EPA lowering the annual $PM_{2.5}$ NAAQS from 12.0 μg/m^3 to 9.0 μg/m^3; as it currently stands, the $PM_{2.5}$ design value for Imperial County is 11.0 μg/m^3 (EPA, 2023), primarily influenced by the Calexico site. To examine trends in $PM_{2.5}$ seasonally and diurnally, data was analyzed from six CARB sites for the years 2014-2023—these years were chosen based on sufficient availability of $PM_{2.5}$ data. After examining monthly average trends, it is apparent that $PM_{2.5}$ exceedances are concentrated on either end of the basin: Banning in the north and the Southern Imperial Valley at the Calexico site. $PM_{2.5}$ monthly averages exceed the annual NAAQS of 9.0 μg/m^3 every month except for March in Calexico (Fig. 5). Aside from late spring/early summer maximum at the Naval Test Base site, Banning is the only other site with monthly averages that exceed the annual NAAQS, and this occurs from March to October, indicating a predominance of photochemical production of secondary aerosols. All other sites attain the annual NAAQS and observe summertime maxima—Calexico is the only site within the valley that observes maximum $PM_{2.5}$ concentrations in the winter. During winter, cold-air pools (CAP) are common in mountain valleys during periods of light wind, high atmospheric pressure, and low insolation and are associated with surface-based temperature inversions (Daly et al., 2009; Lareau et al., 2013). When these stagnant air masses persist, the local emissions from combustion, burning, and any agricultural sources of $PM_{2.5}$ accumulate within the stagnant air (Silcox et al., 2011). Monitoring sites along the Salton Sea (Sonny Bono, Naval Test Base, Bombay Beach, and Torres-Martinez) are maintained by Imperial Irrigation District and are not a part of the U.S. EPA Air Quality System, so long-term trend analysis for $PM_{2.5}$ design values is not reported.

Diurnal profiles of seasonal $PM_{2.5}$ concentrations were also prepared to examine the times which most influence $PM_{2.5}$ exceedances, with reference to the 24-h average NAAQS of 35 μg/m^3 (Fig. 6). Referring to the seasonal diurnal averages (represented by the thick white line), routine exceedances are observed in Mexicali, Mexico during the winter, and to a lesser extent Calexico. In addition, $PM_{2.5}$ maxima were observed in the mornings and evenings as a response to diurnal changes in the mixing height and possibly source timing of cooking, automobile, and heating combustion. Referring to seasonal deviations, Naval Test Base and Sonny Bono, two sites located on the southwestern and southern sides of the Salton Sea, respectively, observe high $PM_{2.5}$ events during spring evenings. This may be related to wind-blown dust that results from strong, late afternoon/evening westerly winds observed in the spring (Fig. 2A), as well as emissions from the Salton Sea and surrounding playa (Evan, 2019; Freedman et al., 2020; Frie et al., 2019). In addition, Calexico observed similar fall/winter diurnal trends with $PM_{2.5}$ compared to the two Mexicali monitoring sites, albeit with lower concentrations. Fig. 7 shows hourly $PM_{2.5}$ deviations from the diurnal

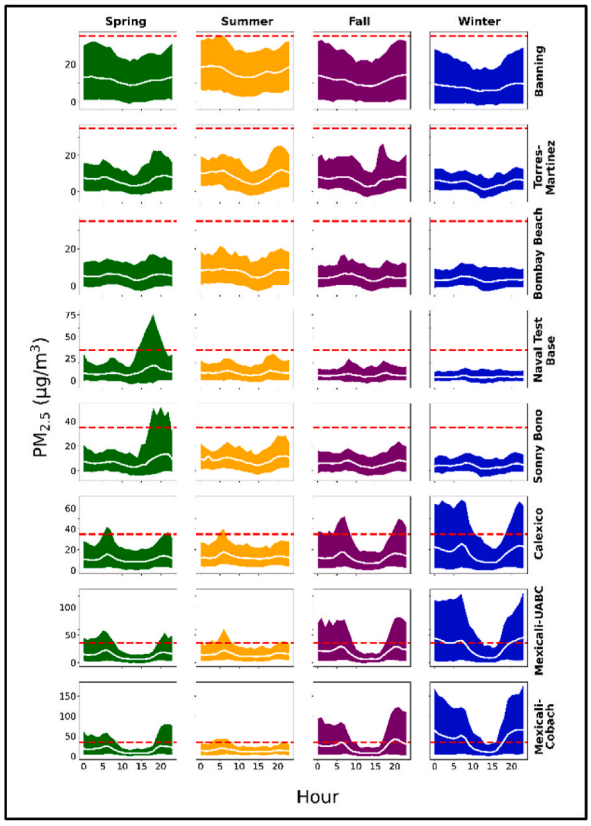

Fig. 6. Seasonal diurnal averages for $PM_{2.5}$ concentrations at each site in the Imperial and Coachella Valleys ($PM_{2.5}$ also includes measurements from Mexicali). Note that the white line represents the seasonal average $PM_{2.5}$ concentration, while the colors represent the upper 95th percentile and lower 5th percentile. The dashed red line represents the NAAQS for 24-h $PM_{2.5}$ concentrations, which should not exceed 35 μg/m^3 (Spring = MAM, Summer = JJA, Fall = SON, Winter = DJF). (For interpretation of the references to color in this figure legend, the reader is referred to the Web version of this article.)

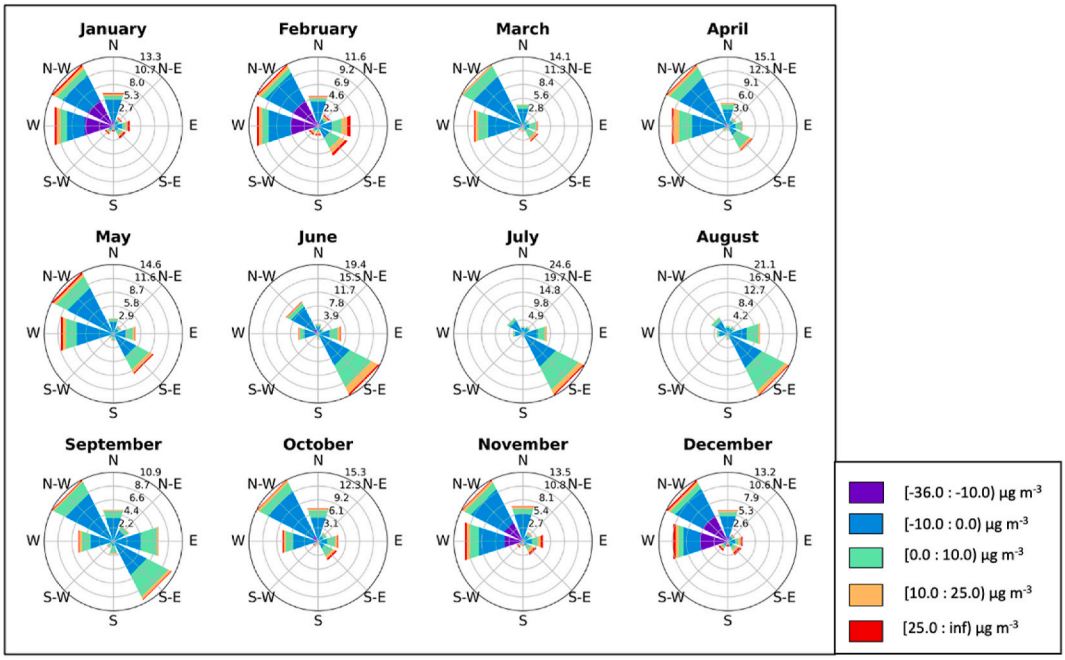

Fig. 7. $PM_{2.5}$ pollution roses for Calexico. The colors represent *hourly $PM_{2.5}$ deviations* from the hourly mean during winds coming from each direction sector. (For interpretation of the references to color in this figure legend, the reader is referred to the Web version of this article.)

mean, where wintertime wind directions are primarily northwesterly, westerly, and northerly. While the more infrequent easterly/southeasterly winds bring elevated $PM_{2.5}$ concentrations, at least as commonly higher than average concentrations are observed in the prevailing northerly-to-westerly wintertime flows. Thus, while Mexicali could be a source for $PM_{2.5}$ production during the wintertime $PM_{2.5}$ events, there is a large and consistent source from winds originating from the US side of the border. Further investigation of regional wind patterns was performed for a concise understanding of interregional air pollution influences in Section 3.

4.4. *Normalized anomalies for $PM_{2.5}$*

Monthly mean normalized anomalies and correlation coefficients were calculated using data from CARB for 2014–2023. Normalized anomalies on days that exceed 24-hr $PM_{2.5}$ NAAQS of 35 µg/m^3 along with SE can be found in Table S5. Since $PM_{2.5}$ exceedances are most concentrated in Calexico and the Naval Test Base site, our analysis will focus on these. In Calexico, average NO_x and PM_{10} concentrations during $PM_{2.5}$ exceedances have very strongly correlated anomalies, as well as the CO and $PM_{2.5}/PM_{10}$ ratio (92nd, 85th, 97th, and 86th percentiles, respectively). Sources of NO_x are likely dominated by combustion processes in the winter however, soil NO_x sources may be an important factor even during the winter months (Lieb et al., 2024). Because of the moderate fall and winter temperatures, the primarily planting season in the Imperial Valley occurs from September to April, meaning that fertilization dominates during this period (Byrnes et al., 2020; Lieb et al., 2024; Watson and Chow, 2001; Yienger and Levy, 1995). Additionally, particulate nitrate on average accounts for 22 % of the 98th percentile $PM_{2.5}$ chemical speciation on these exceedance days (Fig. S7), likely linked to higher-than-average NO_x concentrations. During the winter months, the daytime atmospheric lifetime of NO_x is significantly extended due reduced actinic fluxes. Coupled with abundant ammonia concentrations from agricultural activities and livestock, as well as lower temperatures, the production of particulate nitrate is an important source of wintertime $PM_{2.5}$ (Granella et al., 2024). Source apportionment and chemical speciation of $PM_{2.5}$ in Calexico is discussed further in Section 4.5.

Four of the six $PM_{2.5}$ sites are along the perimeter of the Salton Sea. The first site is in the Northern Imperial Valley in Sonny Bono, and $PM_{2.5}$ exceedances (n = 6) were associated with strong northwesterly winds, higher than average temperatures, and exceptionally high PM_{10} concentrations (wind speed, temperature, and PM_{10} were in the 96th, 76th, and 100th percentiles, respectively). However, with few data points and missing data, these values have a high degree of uncertainty, see Table S5 (SE $\geq$ 0.3). Few exceedance days paired with these normalized anomalies indicate that the $PM_{2.5}$ pollution in Sonny Bono may be a result of exceptional weather events associated with high winds and warm temperatures. Further, there is a strong positive correlation between $PM_{2.5}$ and PM_{10}—these factors, in combination with the normalized anomaly data, may be indicative of meteorological influence on emissive compounds and playa dust from the Salton Sea (Frie et al., 2017). The $PM_{2.5}$ monitor located on the western side of the Salton Sea, at the Naval Test Base, observed 36 exceedances during the period. These exceedances were associated with strong westerly winds and again very high levels of PM_{10}—scalar average wind speed and PM_{10} normalized anomalies were in the 95th and 100th percentiles, respectively. Springtime exceedances (Fig. S2e) dominate because of synoptically forced downslope winds from the Peninsular Range located west of the site (Evan, 2019). It is also worth noting that at sites with wind dominated PM exceedances, the $PM_{2.5}/PM_{10}$ does not seem to change significantly during high events, indicating that both fine and coarse PM are comparably enhanced by aeolian dust. Bombay Beach is a site located on the eastern side of the Salton Sea, however, only 4 exceedances occurred at this site during the timeframe and analysis of normalized anomalies did not produce significant results. Lastly, in Banning, $PM_{2.5}$ exceedances were strongly associated with high humidity and NO_x levels (80th percentile), consistent with secondary aerosol formation in the summer season. Winds in Banning are overwhelmingly westerly during the summer and springtime, situated in the eastern end of the LA basin; therefore, these exceedance days are likely related to interregional transport of urban $PM_{2.5}$ and precursors like NO_x and VOCs.

In summary, the $PM_{2.5}$ exceedance in the SSAB is primarily concentrated in Calexico and results from localized sources due to stagnating conditions. These sources are discussed further in Section 4.5.

Additionally, $PM_{2.5}$ exceedances in regions immediately surrounding the Salton Sea seem to be heavily impacted by strong wind events and high PM_{10} levels. Just upwind of the Coachella Valley, Banning's $PM_{2.5}$ levels are highest in the summertime under the humid conditions affected by interregional transport of urban $PM_{2.5}$ and its precursors (e.g., NO_x and its oxidation products). The causes of $PM_{2.5}$ exceedances in the SSAB seem to vary significantly across the valley, suggesting that mitigation strategies should be tailored to the specific needs of each region.

Several past studies have suggested that both $PM_{2.5}$ (fine) and PM_{10} (coarse) loadings in the Southwestern US may be significantly enhanced by trans-Pacific transport (H. Yu et al., 2012; Y. Yu et al., 2019) and may be rising due to changing climatic conditions (Achakulwisut et al., 2017; Pu and Ginoux, 2017). While these factors likely affect the PM concentrations in the SSAB, they are not very well understood and sporadic by nature thus not easily determined from simple observational analysis. Furthermore, modeling of these impacts also suffers from large uncertainties as climate models are seen to fail to predict the decadal decreases in relative humidity observed throughout the southwestern US (Simpson et al., 2024), and detection of coarse and fine PM trends are not very robust (Achakulwisut et al., 2017; Aryal and Evans, 2022).

4.5. Chemical Speciation Network data analysis: Calexico

The EPA's Chemical Speciation Network (CSN) was utilized to determine the chemical speciation of $PM_{2.5}$ in Calexico, CA—the site that has the most $PM_{2.5}$ exceedance days in the SSAB. To understand how the speciation varies seasonally, Fig. 8 shows the average seasonal chemical speciation for the years 2009–2023. In the winter months (DJF), there is a stronger than average signature of nitrate, while in warmer months, sulfates have a larger contribution. The concentrations of each chemical species can be found in Table S6. The chemical speciation data was also assessed during $PM_{2.5}$ exceedances, shown in Fig. S7. Here, we see that organic carbon (40 %), nitrates (22 %), and soil materials (16 %) comprise the majority of the $PM_{2.5}$ on exceedance days, or when $PM_{2.5}$ concentrations exceed the 24-h NAAQS of 35 μg/m^3. This is approximately consistent with the average wintertime aerosol composition because most exceedance days occur in the winter months.

The NMF analysis yielded five identifiable dominant sources based on factor profiles: (1) biomass burning, (2) motorized vehicle combustion, (3) agricultural soils, (4) industrial, and (5) dust. Factor contribution and profiles were normalized to one and facilitated source apportionment and profile interpretability. Each factor was unique in their elemental composition (Fig. 9), and our analysis was compared to a detailed source characterization study from Watson and Chow (2001). The composition of factor 1 was fairly consistent with their assessment of vegetative burning, with OC as the most abundant species. OC accounted for ~80 % of the total mass and the OC/TC ratio was 0.82, much higher than the ratio for motor vehicle profiles. Sources of biomass burning in the Imperial Valley include agricultural field burning, domestic trash burning, and residential wood combustion, with field burning being the strongest emitter (Watson and Chow, 2001). Aside from OC and EC, other markers of biomass burning mentioned by Watson and Chow (2001) were less than 5 %.

Factor 2's composition was consistent with Watson and Chow

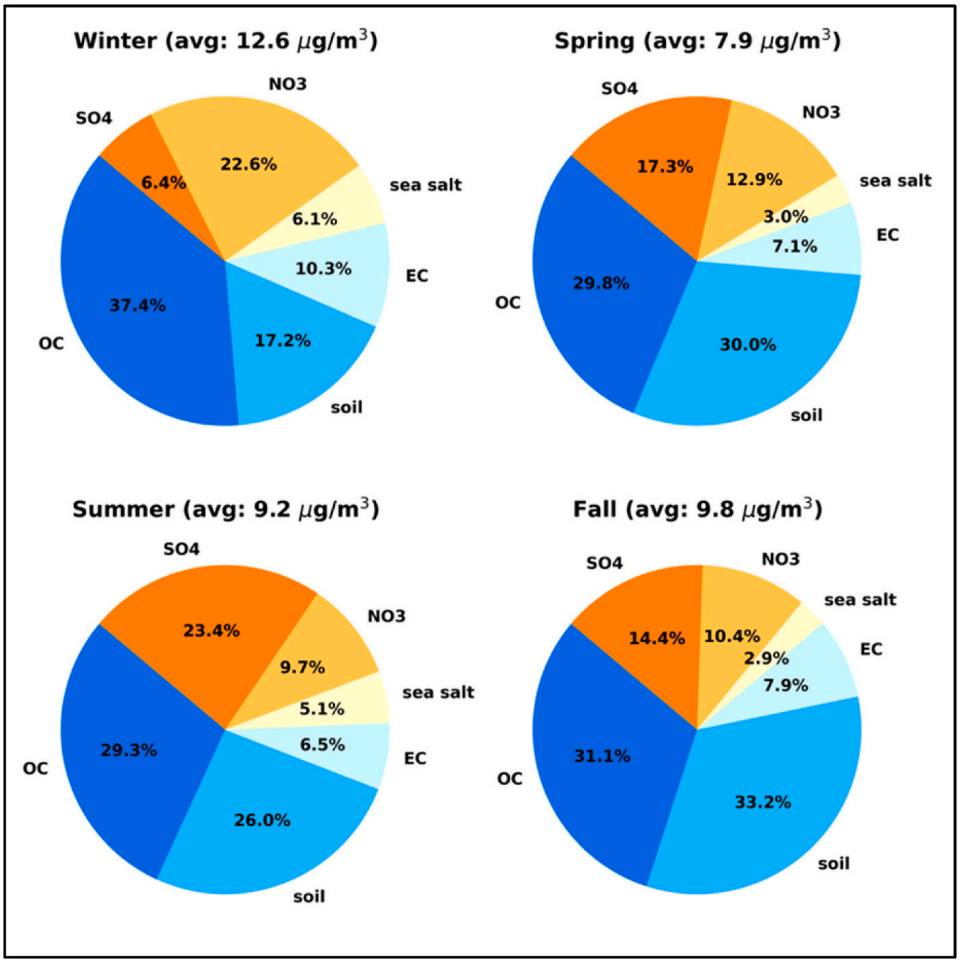

Fig. 8. Chemical speciation of $PM_{2.5}$ in Calexico, CA averaged by season for the years 2009–2023.

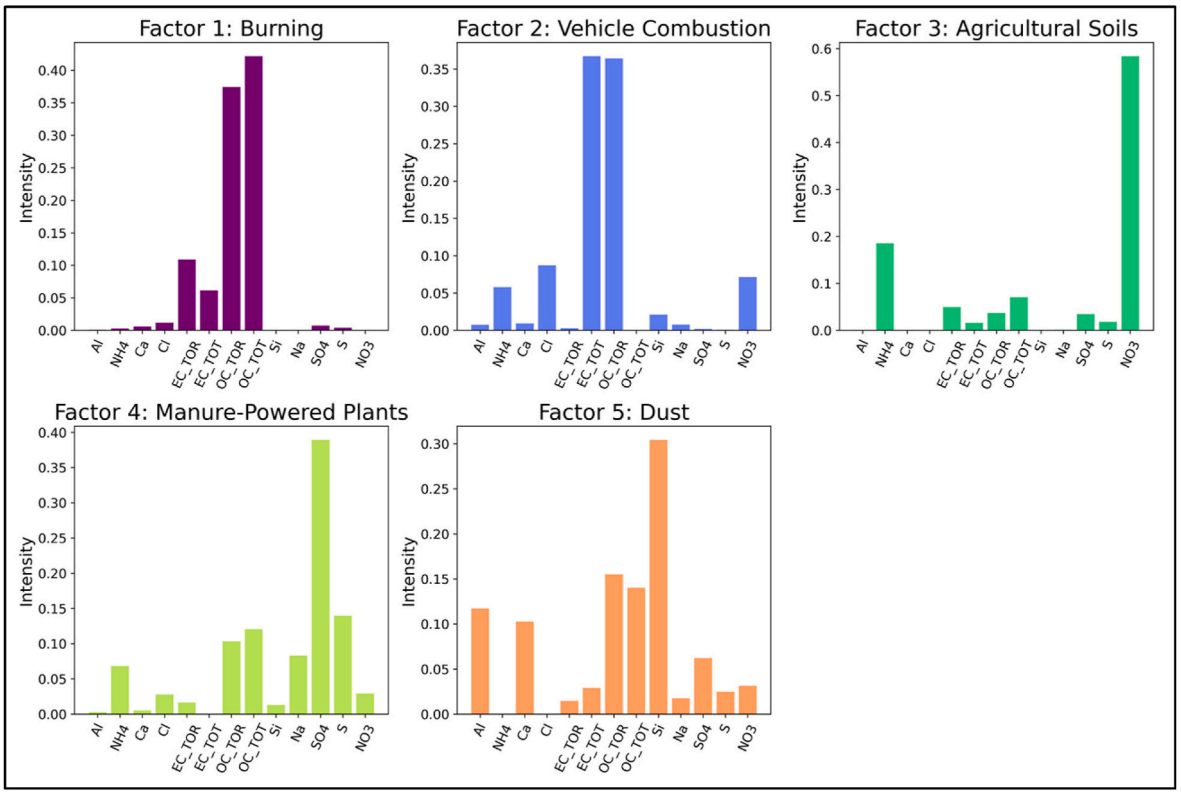

Fig. 9. The relative compositional makeup of the leading 5 factors from a Non-negative Matrix Factorization analysis of the chemical speciation of $PM_{2.5}$ data in Calexico, CA for the years 2009–2023.

(2001)'s analysis of motorized vehicle combustion, although the relative normalized contributions differed. It's important to note that Watson and Chow (2001) analyzed several field samples of data, whereas we are looking at long term factorizations (2009–2023). Markers for motorized vehicle combustion include high contributions of OC, EC, and chlorine. Watson and Chow (2001) observed a strong profile of sulfate; however, we see a larger influence of ammonium nitrate. Factor 3 indicates a large signal of ammonium nitrate and small signatures (<10 %) from EC, OC, sulfur, and sulfate. This profile was not observed in the Watson and Chow (2001) analysis, but due to the approximately 1:3 mass ratio of ammonium to nitrate, we believe that this factor represents particulate ammonium nitrate that originates from heavily-fertilized agricultural soils(Lieb et al., 2024). Imperial County is responsible for over $2 billion in agricultural sales and is ranked 9th in the state, yet it uses more N fertilizer than the top three producing counties combined, resulting in high soil NO_x concentrations that may elevate local particulate nitrate

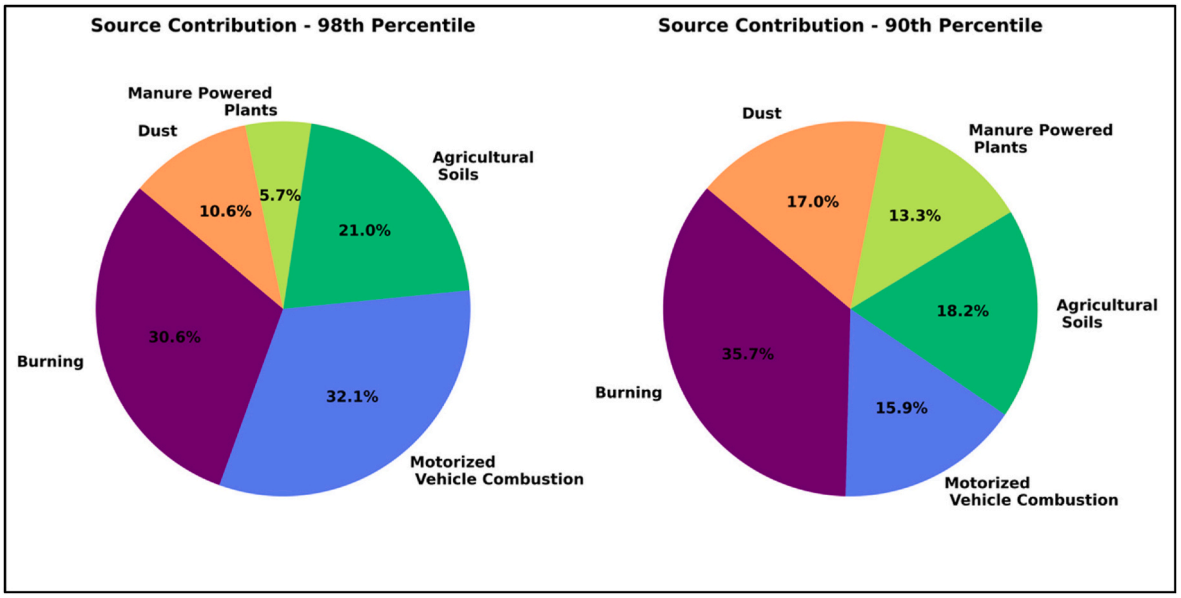

Fig. 10. (A) Shows the source contribution to $PM_{2.5}$ 98th percentile in Calexico, CA. (B) Shows the source contribution to the 90th percentile of $PM_{2.5}$ measurements in Calexico, CA.

concentrations (Lieb et al., 2024). Low concentrations of EC and OC may indicate relatively small contributions from organonitrate and organosulfate compounds.

Furthermore, factor 4 corresponds to Watson and Chow's assessment of industrial source emissions, specifically a manure-fueled power plant located upwind in El Centro, CA. The largest chemical component of factor 4 was sulfate (~39 %), like the contribution measured by Watson and Chow. Lastly, factor 5's strong signatures of silicon (Si), aluminum (Al), and calcium (Ca) are all crustal components that likely indicate a dust source. In addition, organic carbon—a natural component of crustal material—is likely enhanced by road dust and soil sources of crop debris, burn residue, and agricultural chemicals (e.g., pesticides, herbicides, fungicides) (Watson and Chow, 2001).

To assess the contribution of each source to $PM_{2.5}$ exceedance, we selected from the dataset the 98th percentile of high $PM_{2.5}$ days and averaged the factors from the NMF analysis. The results are shown in Fig. 10. Motorized vehicle combustion, biomass burning, and agricultural soil emissions tend to dominate as producers of $PM_{2.5}$ for Calexico. However, because the CSN data is only collected every six days, there are only 12 measurements used to calculate this, thereby increasing the uncertainty of this assessment. To increase the number of data points, we performed a similar analysis for the 90th percentile of the data (n = 80 days), which shows that biomass burning is the dominant source of the upper end of $PM_{2.5}$ concentrations, followed by agricultural soil emissions and dust.

To address the continued nonattainment of $PM_{2.5}$ in Calexico, further work is necessary to reduce the impact of burning, agricultural soil NO_x emissions, and dust entrainment. Additionally, several mitigation strategies can be implemented, including stricter burning regulations, regulations on agricultural practices, and dust control measures. Enforcing stricter burning regulations and the reduction of burning during critical air quality periods may mitigate commercial burning sources, while the conversion to renewable heating sources may reduce residential burning. Extensive procedures on ways to manage agricultural practices have been outlined in Lieb et al. (2025); Lieb et al. (2025). Furthermore, soil stabilizers and vegetative cover in fallow farmlands or around the Salton Sea may reduce dust entrainment and help mitigate wind erosion. By implementing these strategies, Calexico can make significant progress toward achieving $PM_{2.5}$ attainment and improving the health and well-being of its residents.

4.6. PM_{10}

The SSAB is in "Serious" nonattainment for coarse + fine particulate matter (PM_{10}, d ≤ 10 μm), which is typically associated with dust, soot, metals, and salts. PM_{10} is known to have negative health implications due to short and long-term exposure. To analyze trends for annual and diurnal PM_{10} patterns, sites from CARB for the years 2009–2023 were used. Referring to the monthly average trends (Fig. 11A), it is apparent that high PM_{10} concentrations are most frequently observed in Calexico and at the sites surrounding the Salton Sea albeit at different seasonal maxima. Calexico observes maximum levels in the fall, while Sonny Bono and Naval Test Base exhibit a strong peak in April/May. All other sites have a summertime maximum. Because PM_{10} emissions are strongly related to wind speed (Tables S7a and b), it is important to understand the seasonal fluctuations of wind speed that may be influencing these events and ultimately leading to the strong seasonal variability between sites. Seasonal diurnal patterns of PM_{10} at the different sites are shown in Fig. 12. It is apparent that during the spring and summer, every site south of Palm Springs experiences a pronounced peak in PM_{10} concentrations in the late afternoon/early evening (15:00–22:00). Referring to Fig. 2, these events are associated with relatively strong westerly (northwesterly in the Coachella Valley) flow at the culmination of the diurnal thermal forcing as the winds veer to their nocturnal, westerly direction. Wind patterns are discussed in more detail in Section 3 and relationships to wind speed are discussed in Section 4.7.

Further, the long-term PM_{10} design values for the 24-h average NAAQS are shown for available sites in Fig. 11B since the turn of the 21st Century. There is significant variability in the PM_{10} data since exceedances are often associated with extreme meteorological events like windstorms and droughts. In 2020, the EPA approved Imperial County's SIP for PM_{10} attainment, claiming that anthropogenic sources of PM_{10} are being mitigated as to not exceed the PM_{10} standard. However, the two Imperial County sites in Fig. 11B (Niland and Calexico) are currently exceeding the NAAQS, and there does not appear to be any significant long-term diminution trends in PM_{10} DV. Therefore, understanding the factors that exacerbate these exceedances is crucial.

4.7. Normalized anomalies for PM_{10}

Monthly mean normalized anomalies, as well as SE, for PM_{10} exceedance days were calculated using CARB data from 2009 to 2023 and are shown in Tables S7a and b. Correlation coefficients (R^2) were not reported due to their insignificance. There are 4 p.m.$_{10}$ monitors (Table S7a) in Imperial County and four in the Coachella Valley (Table S7b). The sites from the Salton Sea down across the Imperial Valley all share a similar pattern: high wind speeds, primarily westerly in direction, and high $PM_{2.5}$ but low $PM_{2.5}/PM_{10}$ ratios. Calexico, Indio, and Palm Springs exceedances exhibit lower than average NO_x, CO, and (mostly) O_3 concentrations, indicating that combustion sources are likely not contributing to these PM_{10} events, but instead are related to extreme wind events lofting PM from the surface and ventilating trace gas pollutants. Because of this, PM_{10} composition is likely primarily crustal dust material. Dust events are anticipated to become more frequent because of climate change induced drought in the

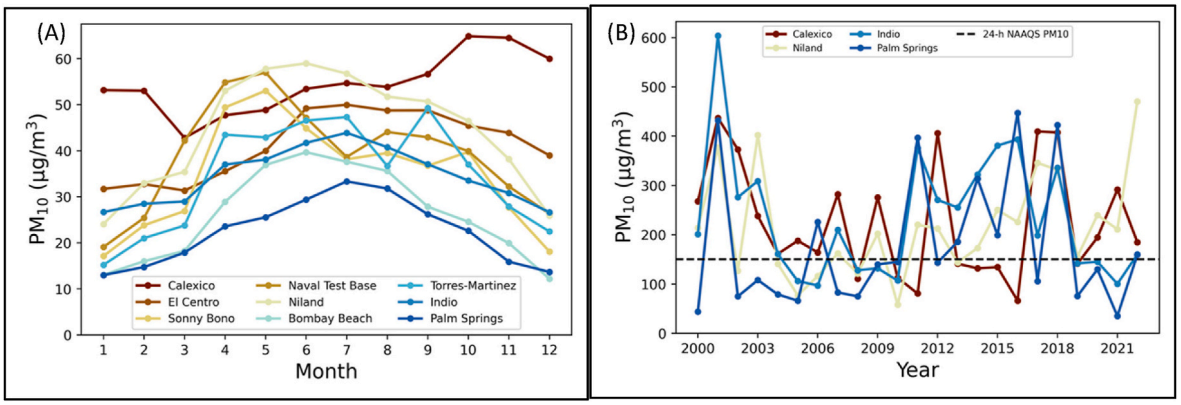

Fig. 11. (A) Monthly mean concentrations of PM_{10} for each of the CARB sites. (B) PM_{10} design values for the 24-h average NAAQS for available sites.

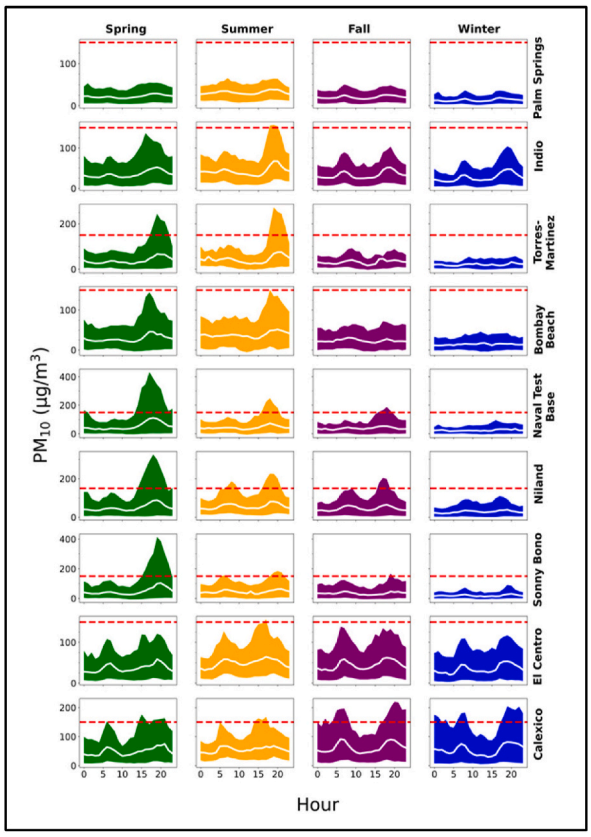

Fig. 12. Seasonal diurnal averages for PM_{10} concentrations at each site in the Imperial and Coachella Valleys. Note that the white line represents the seasonal average PM_{10} concentration, while the colors represent the upper 95th percentile and lower 5th percentile. The dashed red line represents the NAAQS for 24-h $PM_{2.5}$ concentrations, which should not exceed 35 μg/m^3 (Spring = MAM, Summer = JJA, Fall = SON, Winter = DJF). (For interpretation of the references to color in this figure legend, the reader is referred to the Web version of this article.)

Southwestern US (Achakulwisut et al., 2018; NOAA, 2024)

The analysis highlights the complex interplay between meteorological factors and pollutant sources driving PM_{10} concentrations. Understanding these relationships is crucial for developing targeted air quality management strategies. Specific actions might include local emission controls, especially in urban areas where combustion sources likely contribute, as well as dust mitigation strategies, especially surrounding the Salton Sea. Addressing PM_{10} requires a multifaceted approach that includes mitigating dust from agricultural activities and improving land management practices. Furthermore, community engagement and investment in green infrastructure, such as windbreaks and wetland restoration, could help reduce the impact of wind-blown dust in the region (Bradley and Yanega, 2018).

5. Conclusions

This study underscores the multifaceted nature of air quality challenges in the Salton Sea Air Basin (SSAB), where agricultural emissions, wind-driven dust resuspension, and transboundary pollution converge to create persistent exceedances of air quality standards. Additionally, this research provides critical insights into the interplay between meteorological conditions and pollutant sources in a unique and understudied region. Long-term trend analysis and various statistical methods were used to identify key contributors to ozone, $PM_{2.5}$, and PM_{10} pollution, such as unregulated agricultural soil emissions, biomass burning, and wind-driven dust. These findings highlight the urgent need for targeted, evidence-based air quality management strategies that address the specific sources and conditions affecting the SSAB.

Beyond regulatory compliance, mitigating these pollution sources holds broader implications for improving public health, particularly in disadvantaged communities like those in Calexico and those surrounding the Salton Sea, which bear the brunt of these exceedances. Moreover, understanding the dynamics of NO_x-limited ozone production and the role of dust resuspension offers valuable guidance for similar arid and agricultural regions worldwide. By bridging local environmental challenges with broader scientific and policy considerations, this work contributes to advancing equity in air quality management and sustainable agricultural and industrial practices.

CRediT authorship contribution statement

Heather C. Lieb: Writing – review & editing, Writing – original draft, Visualization, Methodology, Investigation, Formal analysis, Data curation. **Ian C. Faloona:** Writing – review & editing, Validation, Supervision, Resources, Project administration, Methodology, Investigation, Funding acquisition, Formal analysis, Conceptualization.

Funding

This work was made possible by support from the University of California, Davis (UC Davis) Environmental Health Sciences Center (EHSC) under award number P30ES023513 of the National Institute of Environmental Health Sciences, National Institute of Health. The content is solely the responsibility of the authors and does not necessarily represent the official views of the UC Davis EHSC, nor the National Institutes of Health. Co-funding was also provided by the Western Center of Agricultural Health and Safety via NIOSH grant [#U54OH007550]. I. C. Faloona's effort was supported by the USDA National Institute of Food and Agriculture, [Hatch project CA-D-LAW-2481-H, "Understanding Background Atmospheric Composition, Regional Emissions, and Transport Patterns Across California"].

Declaration of competing interest

The authors declare that they have no known competing financial interests or personal relationships that could have appeared to influence the work reported in this paper.

Acknowledgements

This work was inspired tremendously by our community partners who provided us with firsthand insight regarding the impacts of the region's meteorology on air pollution events. We would like to acknowledge Comité Cívico del Valle and the Torres Martinez Tribe for working closely with us to learn about community concerns regarding their air quality. In addition, we would like to thank the Imperial County Environmental Justice Task Force and AB617 virtual community meetings for the opportunity to listen and discuss air quality issues with the community. Discussions with colleagues Will Porter and Amato Evan also helped advance this study.

Appendix A. Supplementary data

Supplementary data to this article can be found online at https://doi.org/10.1016/j.atmosenv.2025.121191.

Data availability

Data will be made available on request.

References

Abman, R., Edwards, E.C., Hernandez-Cortes, D., 2024. Water, dust, and environmental justice: the case of agricultural water diversions. Am. J. Agric. Econ. https://doi.org/10.1111/ajae.12472 ajae.12472.

Achakulwisut, P., Mickley, L.J., Anenberg, S.C., 2018. Drought-sensitivity of fine dust in the US Southwest: implications for air quality and public health under future climate change. Environ. Res. Lett. 13 (5), 054025. https://doi.org/10.1088/1748-9326/aabf20.

Achakulwisut, P., Shen, L., Mickley, L.J., 2017. What controls springtime fine dust variability in the western United States? Investigating the 2002–2015 increase in fine dust in the U.S. Southwest. J. Geophys. Res. Atmos. 122 (22), 12449. https://doi.org/10.1002/2017JD027208.

Adams, D.K., Comrie, A.C., 1997. The North American monsoon. Bull. Am. Meteorol. Soc. 78 (10), 2197–2213. https://doi.org/10.1175/1520-0477(1997)078<2197:TNAM>2.0.CO;2.

Al-Hemoud, A., Al-Dousari, A., Al-Shatti, A., Al-Khayat, A., Behbehani, W., Malak, M., 2018. Health impact assessment associated with exposure to PM10 and dust storms in Kuwait. Atmosphere 9 (1), 6. https://doi.org/10.3390/atmos9010006.

Almaraz, M., Bai, E., Wang, C., Trousdell, J., Conley, S., Faloona, I., Houlton, B.Z., 2018. Agriculture is a major source of NO $_x$ pollution in California. Sci. Adv. 4 (1), eaao3477. https://doi.org/10.1126/sciadv.aao3477.

Aryal, Y., Evans, S., 2022. Decreasing trends in the western US dust intensity with rareness of heavy dust events. J. Geophys. Res. Atmos. 127 (13), e2021JD036163. https://doi.org/10.1029/2021JD036163.

Borro, M., Di Girolamo, P., Gentile, G., De Luca, O., Preissner, R., Marcolongo, A., Ferracuti, S., Simmaco, M., 2020. Evidence-based considerations exploring relations between SARS-CoV-2 pandemic and air pollution: involvement of pm2.5-mediated up-regulation of the viral receptor ACE-2. Int. J. Environ. Res. Publ. Health 17 (15), 5573. https://doi.org/10.3390/ijerph17155573.

Bradley, T.J., Yanega, G.M., 2018. Salton Sea: ecosystem in transition. Science 359 (6377), 754. https://doi.org/10.1126/science.aar6088, 754.

Byrnes, D.K., Van Meter, K.J., Basu, N.B., 2020. Long-term shifts in U.S. Nitrogen sources and sinks revealed by the New TREND-nitrogen data set (1930–2017). Glob. Biogeochem. Cycles 34 (9), e2020GB006626. https://doi.org/10.1029/2020GB006626.

Caiazzo, F., Ashok, A., Waitz, I.A., Yim, S.H.L., Barrett, S.R.H., 2013. Air pollution and early deaths in the United States. Part I: quantifying the impact of major sectors in 2005. Atmos. Environ. 79, 198–208. https://doi.org/10.1016/j.atmosenv.2013.05.081.

California Air Resources Board, 2023. *Particulate Matter and health fact sheet.* Particulate matter and health fact sheet. https://ww2.arb.ca.gov/resources/fact-sheets/particulate-matter-and-health-fact-sheet.

California Air Resources Board, 2024a. Air quality data (PST) query tool. https://www.arb.ca.gov/aqmis2/aqdselect.php.

California Air Resources Board, 2024b. Meteorology data query tool (PST). https://www.arb.ca.gov/aqmis2/metselect.php.

California Department of Food and Agriculture, 2023. Fertilizing materials tonnage report 2023. FEED, FERTILIZER, AND LIVESTOCK DRUGS REGULATORY SERVICES DIVISION OF INSPECTION SERVICES.

Carrow, R.N., 1997. Turfgrass response to slow-release nitrogen fertilizers. Agron. J. 89 (3), 491–496. https://doi.org/10.2134/agronj1997.00021962008900030020x.

Dessert, M., 2018a. Imperial County 2018 Redesignation Request and Maintenance Plan for Particulate Matter Less than 10 Microns in Diameter.

Dessert, M., 2018b. IMPERIAL COUNTY 2018 STATE IMPLEMENTATION PLAN (SIP) FOR THE 2012 ANNUALSTANDARD FOR PARTICULATE MATTER LESS THAN 2.5 MICRONS IN DIAMETER (2018 ANNUAL PM2.5 SIP).

D'Evelyn, S.M., Vogel, C.F.A., Bein, K.J., Lara, B., Laing, E.A., Abarca, R.A., Zhang, Q., Li, L., Li, J., Nguyen, T.B., Pinkerton, K.E., 2021. Differential inflammatory potential of particulate matter (PM) size fractions from imperial valley, CA. Atmos. Environ. 244, 117992. https://doi.org/10.1016/j.atmosenv.2020.117992.

Dominici, F., Peng, R.D., Bell, M.L., Pham, L., McDermott, A., Zeger, S.L., Samet, J.M., 2006. Fine particulate air pollution and hospital admission for cardiovascular and respiratory diseases. JAMA 295 (10), 1127. https://doi.org/10.1001/jama.295.10.1127.

EPA, 2022. Determination of attainment by the attainment date but for international emissions for the 2015 ozone national ambient air quality standard; imperial county, California. Fed. Regist. https://www.federalregister.gov/documents/2022/10/20/2022-22276/determination-of-attainment-by-the-attainment-date-but-for-international-emissions-for-the-2015.

EPA, 2023. Determination of attainment by the attainment date, clean data determination, and approval of Base year emissions inventory for the imperial county, California nonattainment area for the 2012 annual fine particulate matter NAAQS. Fed. Regist. https://www.federalregister.gov/documents/2023/01/11/2022-28278/determination-of-attainment-by-the-attainment-date-clean-data-determination-and-approval-of-base.

EPA, 2024. Final Rule to Strengthen the National Air Quality Health Standard for Patriculate Matter.

Evan, A.T., 2019. Downslope winds and dust storms in the Salton basin. Mon. Weather Rev. 147 (7), 2387–2402. https://doi.org/10.1175/MWR-D-18-0357.1.

Freedman, F.R., English, P., Wagner, J., Liu, Y., Venkatram, A., Tong, D.Q., Al-Hamdan, M.Z., Sorek-Hamer, M., Chatfield, R., Rivera, A., Kinney, P.L., 2020. Spatial particulate fields during high winds in the Imperial Valley, California. Atmosphere 11 (1), 88. https://doi.org/10.3390/atmos11010088.

Frie, A.L., Dingle, J.H., Ying, S.C., Bahreini, R., 2017. The effect of a receding saline lake (the Salton Sea) on airborne particulate matter composition. Environ. Sci. Technol. 51 (15), 8283–8292. https://doi.org/10.1021/acs.est.7b01773.

Frie, A.L., Garrison, A.C., Schaefer, M.V., Bates, S.M., Botthoff, J., Maltz, M., Ying, S.C., Lyons, T., Allen, M.F., Aronson, E., Bahreini, R., 2019. Dust sources in the Salton Sea basin: a clear case of an anthropogenically impacted dust budget. Environ. Sci. Technol. 53 (16), 9378–9388. https://doi.org/10.1021/acs.est.9b02137.

Garcia, E., Marian, B., Chen, Z., Li, K., Lurmann, F., Gilliland, F., Eckel, S.P., 2022. Long-term air pollution and COVID-19 mortality rates in California: findings from the Spring/Summer and Winter surges of COVID-19. Environ. Pollut. 292, 118396. https://doi.org/10.1016/j.envpol.2021.118396.

Granella, F., Renna, S., Aleluia Reis, L., 2024. The formation of secondary inorganic aerosols: a data-driven investigation of Lombardy's secondary inorganic aerosol problem. Atmos. Environ. 327, 120480. https://doi.org/10.1016/j.atmosenv.2024.120480.

Hao, Y., Balluz, L., Strosnider, H., Wen, X.J., Li, C., Qualters, J.R., 2015. Ozone, fine particulate matter, and chronic lower respiratory disease mortality in the United States. Am. J. Respir. Crit. Care Med. 192 (3), 337–341. https://doi.org/10.1164/rccm.201410-1852OC.

Heuss, J.M., Kahlbaum, D.F., Wolff, G.T., 2003. Weekday/weekend ozone differences: what can we learn from them? J. Air Waste Manag. Assoc. 53 (7), 772–788. https://doi.org/10.1080/10473289.2003.10466227.

Hopke, P.K., 2016. Review of receptor modeling methods for source apportionment. J. Air Waste Manag. Assoc. 66 (3), 237–259. https://doi.org/10.1080/10962247.2016.1140693.

Institute for Health Metrics and Evaluation, 2021. Air pollution. https://www.healthdata.org/research-analysis/health-risks-issues/air-pollution.

Johnston, J.E., Razafy, M., Lugo, H., Olmedo, L., Farzan, S.F., 2019. The disappearing Salton Sea: a critical reflection on the emerging environmental threat of disappearing saline lakes and potential impacts on children's health. Sci. Total Environ. 663, 804–817. https://doi.org/10.1016/j.scitotenv.2019.01.365.

Jones, B.A., Fleck, J., 2020. Shrinking lakes, air pollution, and human health: evidence from California's Salton Sea. Sci. Total Environ. 712, 136490. https://doi.org/10.1016/j.scitotenv.2019.136490.

Kerr, G.H., Waugh, D.W., Strode, S.A., Steenrod, S.D., Oman, L.D., Strahan, S.E., 2019. Disentangling the drivers of the summertime ozone-temperature relationship over the United States. J. Geophys. Res. Atmos. 124 (19), 10503–10524. https://doi.org/10.1029/2019JD030572.

Kim, S.-Y., Kim, E., Kim, W.J., 2020. Health effects of ozone on respiratory diseases. Tuberc. Respir. Dis. 83 (Suppl. 1), S6–S11. https://doi.org/10.4046/trd.2020.0154.

Li, H., Tatarko, J., Kucharski, M., Dong, Z., 2015. PM2.5 and PM10 emissions from agricultural soils by wind erosion. Aeolian Research 19, 171–182. https://doi.org/10.1016/j.aeolia.2015.02.003.

Lieb, H.C., Maldonado, M., Ruiz, E., Torres, C., Olmedo, L., Walters, W.W., Faloona, I.C., 2024. Nitrogen isotopes reveal high NOx emissions from arid agricultural soils in the Salton Sea Air Basin. Sci. Rep. 14 (1), 28725. https://doi.org/10.1038/s41598-024-78361-y.

Lieb, H.C., Rose, M., Amsalem, G., Torres, C., Olmedo, L., Faloona, I.C., 2025. Investigating the impact of soil NOx on air quality in rural agricultural communities: a call to action for environmental justice in California. Environ. Justice. https://doi.org/10.1089/env.2024.0051.

Luo, L., Ran, L., Rasool, Q.Z., Cohan, D.S., 2022. Integrated modeling of U.S. Agricultural soil emissions of reactive nitrogen and associated impacts on air pollution, health, and climate. Environ. Sci. Technol. 56 (13), 9265–9276. https://doi.org/10.1021/acs.est.1c08660.

Madl, A.K., Carosino, C., Pinkerton, K.E., 2010. Particle toxicities. In: Comprehensive Toxicology. Elsevier, pp. 421–451. https://doi.org/10.1016/B978-0-08-046884-6.00923-4.

Malm, W.C., Hand, J.L., 2007. An examination of the physical and optical properties of aerosols collected in the IMPROVE program. Atmos. Environ. 41 (16), 3407–3427. https://doi.org/10.1016/j.atmosenv.2006.12.012.

Marian, B., Yan, Y., Chen, Z., Lurmann, F., Li, K., Gilliland, F., Eckel, S.P., Garcia, E., 2022. Independent associations of short- and long-term air pollution exposure with COVID-19 mortality among Californians. Environmental Advances 9, 100280. https://doi.org/10.1016/j.envadv.2022.100280.

Marr, L.C., Harley, R.A., 2002. Modeling the effect of Weekday−Weekend differences in motor vehicle emissions on photochemical air pollution in central California. Environ. Sci. Technol. 36 (19), 4099–4106. https://doi.org/10.1021/es020629x.

Mendoza, A., Pardo, E.I., Gutierrez, A.A., 2010. Chemical characterization and preliminary source contribution of fine particulate matter in the Mexicali/Imperial Valley border area. J. Air Waste Manag. Assoc. 60 (3), 258–270. https://doi.org/10.3155/1047-3289.60.3.258.

NOAA, 2024. National integrated drought information system. https://www.drought.gov/states/california.

OEHHA, 2023. CalEnviroScreen 4.0. OEHHA. https://oehha.ca.gov/calenviroscreen/report/calenviroscreen-40.

Oikawa, P.Y., Ge, C., Wang, J., Eberwein, J.R., Liang, L.L., Allsman, L.A., Grantz, D.A., Jenerette, G.D., 2015. Unusually high soil nitrogen oxide emissions influence air quality in a high-temperature agricultural region. Nat. Commun. 6 (1), 8753. https://doi.org/10.1038/ncomms9753.

Pacific Institute, 2024. Current information on the Salton Sea. Pacific Institute. https://pacinst.org/current-information-salton-sea/.

Parrish, D.D., Faloona, I.C., Derwent, R.G., 2024. Maximum ozone concentrations in the southwestern US and Texas: implications of growing predominance of background contribution. https://doi.org/10.5194/egusphere-2024-342.

Parrish, D.D., Faloona, I.C., Derwent, R.G., 2025. Maximum ozone concentrations in the southwestern US and Texas: implications of the growing predominance of the background contribution. Atmos. Chem. Phys. 25 (1), 263–289. https://doi.org/10.5194/acp-25-263-2025.

Parrish, D.D., Young, L.M., Newman, M.H., Aikin, K.C., Ryerson, T.B., 2017. Ozone design values in southern California's air basins: temporal evolution and U.S. Background contribution. J. Geophys. Res. Atmos. 122 (20). https://doi.org/10.1002/2016JD026329.

Porter, W.C., Heald, C.L., 2019. The mechanisms and meteorological drivers of the summertime ozone–temperature relationship. Atmos. Chem. Phys. 19 (21), 13367–13381. https://doi.org/10.5194/acp-19-13367-2019.

Pu, B., Ginoux, P., 2017. Projection of American dustiness in the late 21st century due to climate change. Sci. Rep. 7 (1), 5553. https://doi.org/10.1038/s41598-017-05431-9.

Roelofs, G.-J., Lelieveld, J., 1997. Model study of the influence of cross-tropopause O3 transports on tropospheric O3 levels. Tellus B 49 (1), 38–55. https://doi.org/10.1034/j.1600-0889.49.issue1.3.x.

Sha, T., Ma, X., Zhang, H., Janechek, N., Wang, Y., Wang, Y., Castro García, L., Jenerette, G.D., Wang, J., 2021. Impacts of soil NO $_x$ emission on O $_3$ air quality in rural California. Environ. Sci. Technol. 55 (10), 7113–7122. https://doi.org/10.1021/acs.est.0c06834.

Shi, C., Fernando, H.J.S., Yang, J., 2009. Contributors to ozone episodes in three U.S./Mexico border twin-cities. Sci. Total Environ. 407 (18), 5128–5138. https://doi.org/10.1016/j.scitotenv.2009.05.046.

Simpson, I.R., McKinnon, K.A., Kennedy, D., Lawrence, D.M., Lehner, F., Seager, R., 2024. Observed humidity trends in dry regions contradict climate models. Proc. Natl. Acad. Sci. 121 (1), e2302480120. https://doi.org/10.1073/pnas.2302480120.

Škerlak, B., Sprenger, M., Wernli, H., 2014. A global climatology of stratosphere–troposphere exchange using the ERA-Interim data set from 1979 to 2011. Atmos. Chem. Phys. 14 (2), 913–937. https://doi.org/10.5194/acp-14-913-2014.

Stevenson, D.S., Dentener, F.J., Schultz, M.G., Ellingsen, K., Van Noije, T.P.C., Wild, O., Zeng, G., Amann, M., Atherton, C.S., Bell, N., Bergmann, D.J., Bey, I., Butler, T., Cofala, J., Collins, W.J., Derwent, R.G., Doherty, R.M., Drevet, J., Eskes, H.J., et al., 2006. Multimodel ensemble simulations of present-day and near-future tropospheric ozone. J. Geophys. Res. Atmos. 111 (D8). https://doi.org/10.1029/2005JD006338, 2005JD006338.

The New York Times, 2023. California coronavirus map and case count. The New York Times. https://www.nytimes.com/interactive/2023/us/california-covid-cases.html.

Trousdell, J.F., Caputi, D., Smoot, J., Conley, S.A., Faloona, I.C., 2019. Photochemical production of ozone and emissions of NOx and CH4 in the san joaquin valley. Atmos. Chem. Phys. 19 (16), 10697–10716. https://doi.org/10.5194/acp-19-10697-2019.

US EPA, 2016. Chemical speciation network [data and tools]. https://www.epa.gov/outdoor-air-quality-data/interactive-map-air-quality-monitors.

Wang, Y., Faloona, I.C., Houlton, B.Z., 2023. Satellite NO $_2$ trends reveal pervasive impacts of wildfire and soil emissions across California landscapes. Environ. Res. Lett. 18 (9), 094032. https://doi.org/10.1088/1748-9326/acec5f.

Wang, Y., Ge, C., Castro Garcia, L., Jenerette, G.D., Oikawa, P.Y., Wang, J., 2021. Improved modelling of soil NO $_x$ emissions in a high temperature agricultural region: role of background emissions on NO $_2$ trend over the US. Environ. Res. Lett. 16 (8), 084061. https://doi.org/10.1088/1748-9326/ac16a3.

Watson, J.G., Chow, J.C., 2001. Source Characterization of Major Emission Sources in the Imperial and Mexicali Valleys along the USrMexico Border.

Wu, K., Zhu, S., Mac Kinnon, M., Samuelsen, S., 2023. Unexpected deterioration of O3 pollution in the South Coast Air Basin of California: the role of meteorology and emissions. Environ. Pollut. 330, 121728. https://doi.org/10.1016/j.envpol.2023.121728.

Yienger, J.J., Levy, H., 1995. Empirical model of global soil-biogenic NO $_\chi$ emissions. J. Geophys. Res. Atmos. 100 (D6), 11447–11464. https://doi.org/10.1029/95JD00370.

Yu, H., Remer, L.A., Chin, M., Bian, H., Tan, Q., Yuan, T., Zhang, Y., 2012. Aerosols from overseas rival domestic emissions over north America. Science 337 (6094), 566–569. https://doi.org/10.1126/science.1217576.

Yu, Y., Kalashnikova, O.V., Garay, M.J., Notaro, M., 2019. Climatology of Asian dust activation and transport potential based on MISR satellite observations and trajectory analysis. Atmos. Chem. Phys. 19 (1), 363–378. https://doi.org/10.5194/acp-19-363-2019.

Zhang, L., Lin, M., Langford, A.O., Horowitz, L.W., Senff, C.J., Klovenski, E., Wang, Y., Alvarez Ii, R.J., Petropavlovskikh, I., Cullis, P., Sterling, C.W., Peischl, J., Ryerson, T. B., Brown, S.S., Decker, Z.C.J., Kirgis, G., Conley, S., 2020. Characterizing sources of high surface ozone events in the southwestern US with intensive field measurements and two global models. Atmos. Chem. Phys. 20 (17), 10379–10400. https://doi.org/10.5194/acp-20-10379-2020.